

Internet Electronic Journal of Molecular Design

March 2004, Volume 3, Number 3, Pages 110–117

Editor: Ovidiu Ivanciuc

Special issue dedicated to Professor Nenad Trinajstić on the occasion of the 65th birthday
Part 9

Guest Editor: Douglas J. Klein

Structure of Radical Cationic Hydrocarbon $C_3H_5^{2+}$

Iris A. Howard,¹ Norman H. March,^{1,2} and Christian Van Alsenoy³

¹ Department of Physics, University of Antwerp, Groenenborgerlaan 171, B–2020 Antwerp,
Belgium

² Oxford University, Oxford, England

³ Department of Chemistry, University of Antwerp, Universiteitsplein 1, B–2610 Antwerp, Belgium

Received: October 17, 2003; Revised: January 26, 2004; Accepted: February 5, 2004; Published: March 31, 2004

Citation of the article:

I. A. Howard, N. H. March, and C. Van Alsenoy, Structure of Radical Cationic Hydrocarbon $C_3H_5^{2+}$, *Internet Electron. J. Mol. Des.* **2004**, *3*, 110–117, <http://www.biochempress.com>.

Structure of Radical Cationic Hydrocarbon $C_3H_5^{2+\bullet}$

Iris A. Howard,^{1,*} Norman H. March,^{1,2} and Christian Van Alsenoy³

¹ Department of Physics, University of Antwerp, Groenenborgerlaan 171, B–2020 Antwerp, Belgium

² Oxford University, Oxford, England

³ Department of Chemistry, University of Antwerp, Universiteitsplein 1, B–2610 Antwerp, Belgium

Received: October 17, 2003; Revised: January 26, 2004; Accepted: February 5, 2004; Published: March 31, 2004

Internet Electron. J. Mol. Des. 2004, 3 (3), 110–117

Abstract

Motivation. After recent studies on cationic clusters of hydrogen isotopes, we here present results for the cationic hydrocarbon $C_3H_5^{2+\bullet}$ radical.

Method. Hartree–Fock plus low–order Møller–Plesset (MP) perturbation theory are used in computations.

Results. We find a nonlinear, nonplanar ground–state geometry at MP4 level. All normal mode frequencies are real.

Conclusions. The ground–state geometry we find is different from that of recent work (K. Gluch *et al.*, *J. Chem. Phys.* 2003, 118, 3090). At MP4 level, our predicted geometry is lower in energy by approximately 0.26 eV than that of a linear structure. Some comments are made concerning Coulomb explosion of cationic hydrocarbons.

Keywords. Hydrocarbon; Coulomb explosion; radical dication; *ab initio*.

Abbreviations and notations

HF, Hartree–Fock

MP2, second–order Møller–Plesset

MP, Møller–Plesset

MP4, fourth–order Møller–Plesset

1 INTRODUCTION

In earlier work we have studied cationic clusters of hydrogen isotopes. More specifically, the experimental study of the liquid–vapour region of the cluster $H_3^+(H_2)_m$ with $2 \leq m \leq 14$ by Gobet [1], and related observation of negative specific heat, prompted us to study the ground–state geometry, and the electronic structure, for a number of values of m [2]. The method employed was the Hartree–Fock approximation, supplemented by low–order Møller–Plesset perturbation theory. Again prompted by experiment [3], we have subsequently investigated the Coulomb explosion of cationic deuterium clusters [4] using the same approach.

The present study has been motivated by the recent work of Gluch *et al.* [5], who were

Dedicated to Professor Nenad Trinajstić on the occasion of the 65th birthday.

* Correspondence author; E–mail: howard@ruca.ua.ac.be.

concerned with the doubly charged hydrocarbon C₃H₅^{2+•}. The outline of our work is as follows. Section 2 is a brief comment on the computation approach used in the paper. Section 3 consists of a presentation of our results on the geometry and electronic structure of this cationic hydrocarbon, with comparison made with the singly charged species. A study of the vibrational frequencies of the cluster is also reported. A summary is given in section 4, where some possible directions for further studies are suggested.

2 MATERIALS AND METHODS

Using the Hartree–Fock (HF) approximation plus MP corrections, as implemented in GAUSSIAN 98 [6], we have optimized the geometry of five possible structures of C₃H₅^{2+•}, with both the 6–31G** and 6–31+G** bases. With the 6–31G** basis, optimization was carried out up to MP2 level for both multiplicity 2 (S = 1/2) and multiplicity 4 (S = 3/2). Finally, for geometries determined at MP4(SDQ)/6–31+G** level on the low–multiplicity structures, a single–point energy calculation was carried out at MP4(SDQ)/aug–cc–pVTZ level.

3 RESULTS AND DISCUSSION

3.1 Geometry and Electronic Structure of Cationic Hydrocarbon C₃H₅^{2+•}, Compared with Singly–Charged Cation

Results of optimization of the three lowest–energy structures are summarized in Table 1. Structure **1** is linear; structure **2** has a C–C–C bond angle of approximately 120 degrees and is terminated by an ethyl group at each end; structure **3** has nearly the same C–C–C bond angle, but has a CH₂–CH₂–CH structure. Unconstrained optimizations were carried out for both +1 and +2 charge states, for comparison, and in the +2 charge state, for multiplicities of both 2 and 4. Subsequent normal–mode frequency calculations were carried out to check the stability of the energetic minimum.

Table 1. C₃H₅^{q+} Energies (a.u.) at Optimized Geometry

	1	2	3
	<i>q</i> = 2		
HF, 6–31G**	–115.5713	–115.6095	–115.5710
HF, 6–31+G**	–115.5723	–115.6106	–115.5720
HF, 6–31G**, S=3/2	–115.4805 #	–115.4765	–115.4477
MP2, 6–31G**	–115.9191	–115.9276	–115.8869
MP2, 6–31G**, S=3/2	–115.7860 #	–115.7588	–115.7515
MP2, 6–31+G**	–115.9207	–115.9294	–115.8885
MP4, 6–31+G**	–115.9591	–115.9738	–115.9312
	<i>q</i> = 1		
HF, 6–31G**	–116.1764	–116.2021	–116.0448 #
MP2, 6–31G**	–116.5588	–116.5811	–116.3956 #

indicates at least one imaginary frequency; minimum not stable

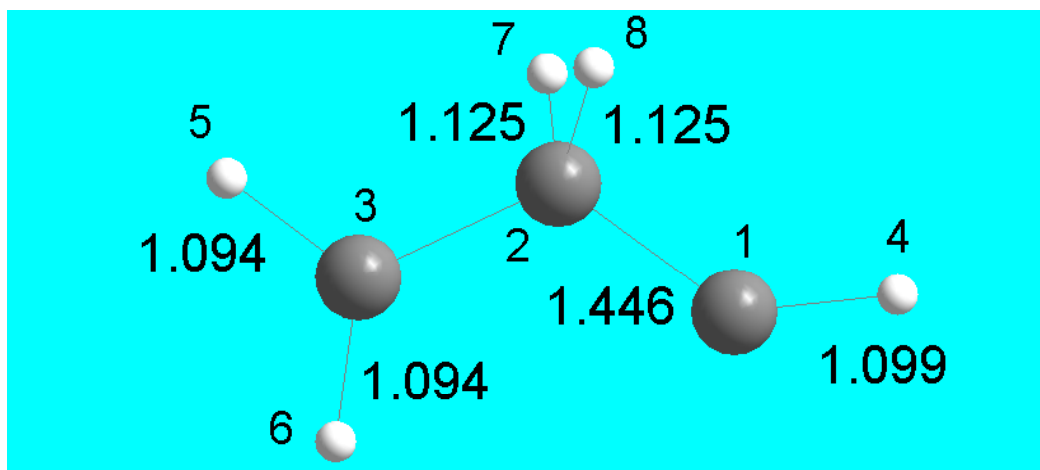
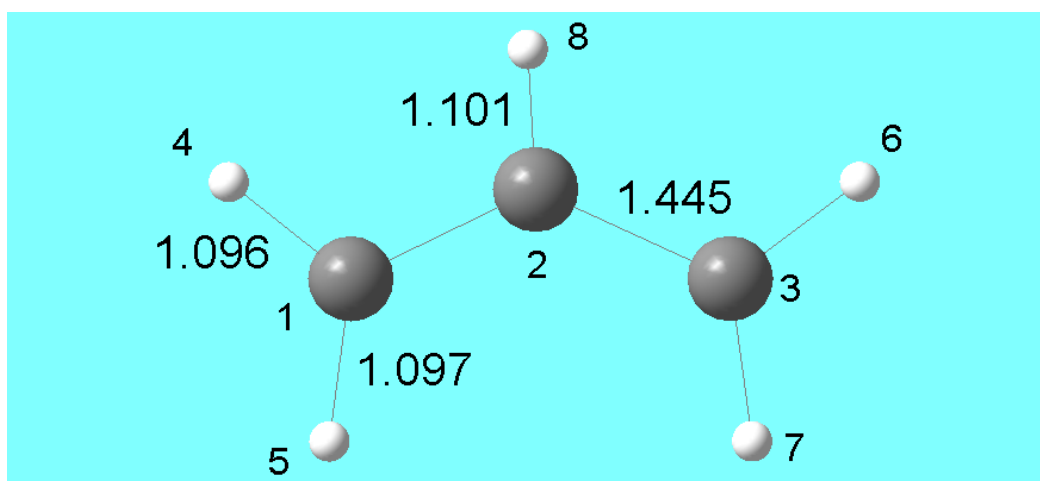
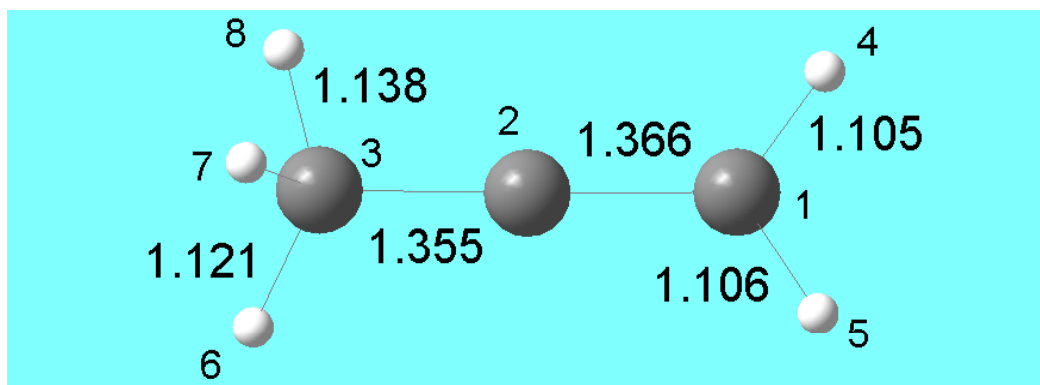


Figure 1. Optimized geometries at MP4 level, with the 6-31+G** basis, for structures 1 (linear), 2 and 3. All distances are in Ångstroms.

For the +2 charge state, we may summarize the results by saying that at HF level, the lowest energy stable minimum is found for structure 2 with multiplicity 2; at MP4 level, this structure again has a stable minimum 0.40 eV below that of structure 1 (the linear structure considered in the earlier work in Ref. [5], and 1.16 eV below the minimum of structure 3, when the 6-31+G** basis

is used. Optimized geometries at this level are shown for all three structures in Figure 1.

Note that the optimized ground state structure **2** is nonplanar at all levels of calculation (see the side view in Figure 2), with a C–C bond length which varies from 1.454 Å at HF level to 1.439 Å at MP2 level, to 1.445 Å at MP4, with the 6–31+G** basis; the C–C–C bond angle at MP4 optimized level is 122.1°.

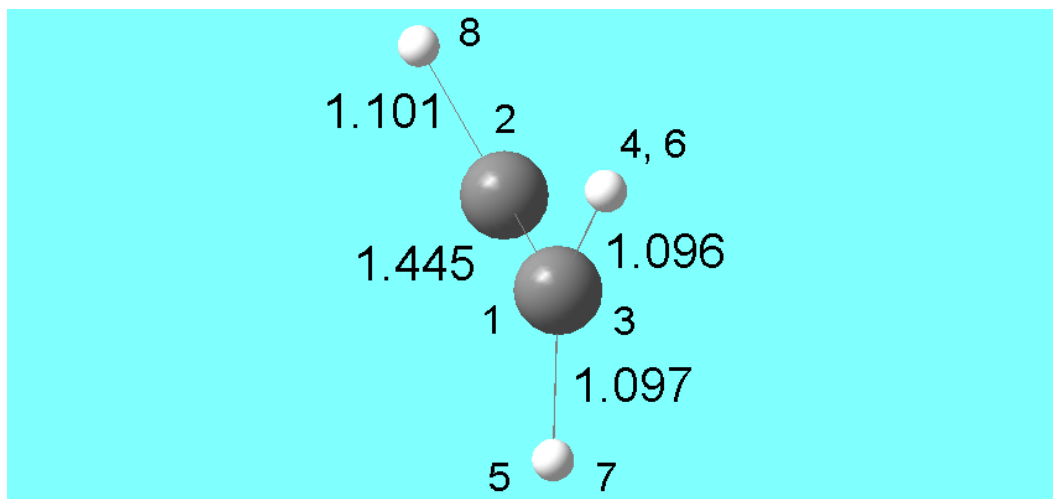


Figure 2. Side view of structure **2** with nonplanar optimized geometry.

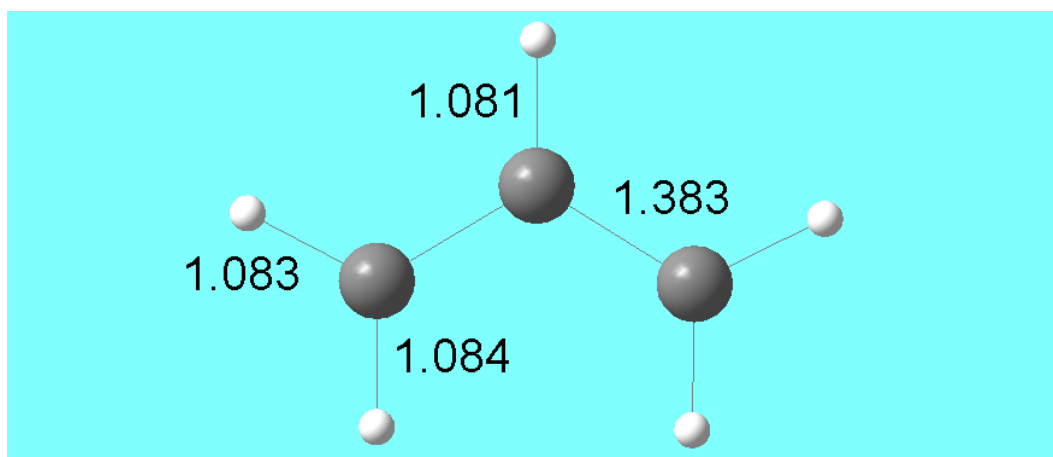


Figure 3. Optimized geometry of $C_3H_5^{1+}$ at MP2 level with the 6-31G** basis; note that this structure, analogous to that of structure **2** for $C_3H_5^{2+}$, is planar.

Two additional stable but higher-energy structures of charge +2, not listed in Table 1, were also considered: the propenyl radical dication $CH_3-CH=CH^{2+}$ (structure **4**) and the cyclopropyl radical dication $-CH_2-CH_2-CH^{2+}$ (structure **5**). As a more accurate check on the energetic ordering of all five structures, we carried out a single-point MP4(SDQ)/aug-cc-pVTZ calculation for each, at the minimum-energy geometry determined at MP4(SDQ)/6–31+G** level. We find the energies at MP4(SDQ)/aug-cc-pVTZ level to be –116.0604 a.u. (structure **1**), –116.0698 a.u. (structure **2**), –116.0273 a.u. (structure **3**), –116.0162 (structure **4**), and –115.9636 a.u. (structure **5**); thus structure

2 lies 0.26 eV below structure **1** at this level of calculation.

Table 2. Mulliken Charges for the Ground-State Structure **2** with Charge +2, $C_3H_5^{2+}$, and the 6–31+G** Basis Set

atom	HF	MP2	MP4
1 C	0.122	0.128	0.108
2 C	0.012	−0.032	0.039
3 C	0.122	0.128	0.108
4 H	0.351	0.355	0.349
5 H	0.337	0.341	0.336
6 H	0.351	0.355	0.349
7 H	0.337	0.341	0.336
8 H	0.370	0.385	0.375

Table 3. Mulliken charges at MP4 level and 6–31+G** basis for the optimized structures **1–3** with charge +2, $C_3H_5^{2+}$

atom	1	2	3
1 C	0.101	0.108	0.451
2 C	0.397	0.039	−0.531
3 C	−0.437	0.108	0.247
4 H	0.382	0.349	0.362
5 H	0.383	0.336	0.338
6 H	0.392	0.349	0.330
7 H	0.392	0.336	0.401
8 H	0.390	0.375	0.401

Table 4. Atomic spin densities for Mulliken and Stockholder partitioning for $C_3H_5^{2+}$

structure	atom number	Mulliken	Stockholder
1	1 C	0.454	0.413
	2 C	0.641	0.471
	3 C	−0.185	0.029
	4 H	−0.018	0.007
	5 H	−0.019	0.007
	6 H	0.065	0.038
	7 H	0.065	0.038
	8 H	−0.003	−0.004
2	1 C	0.085	0.170
	2 C	0.754	0.575
	3 C	0.085	0.170
	4 H	−0.002	0.009
	5 H	0.023	0.016
	6 H	−0.002	0.009
	7 H	0.023	0.016
	8 H	0.035	0.034
3	1 C	1.000	0.866
	2 C	−0.058	0.048
	3 C	0.016	0.019
	4 H	0.000	0.037
	5 H	−0.005	−0.001
	6 H	0.004	0.004
	7 H	0.021	0.014
	8 H	0.021	0.014

For comparison, we consider the optimized geometries, for the three lowest-energy structures, with a net charge of +1. From Table 1, we see that at both the HF and MP2 levels considered, using

the 6–31G** basis, structure **2** is again the lowest in energy; the ground–state structure **2** is now, however, planar, as shown in Figure 3, with a C–C bond length of 1.383 Å and a C–C–C bond angle of 117.5°.

In Table 2 we show the Mulliken atomic charges calculated for the ground–state structure **2**, with charge +2 and the 6–31+G** basis set, for the optimized geometries found at HF, MP2 and MP4 levels. Atomic labeling is as in Figure 1.

We see that at all levels of calculation, the positive charge is carried primarily on the hydrogens, the central carbon in particular being almost neutral. This arrangement of charge is in fact not particular to this structure; the Mulliken charges at MP4 level for the optimized structures **1–3** with charge +2 are compared in Table 3, where we see that the hydrogens in each case carry most of the positive charge.

Finally, atomic spin densities have been generated from the MP4(SDQ)/aug–cc–cPTV results, using both Mulliken and Stockholder partitioning, and are listed in Table 4. We see that the two forms of partitioning give in this case very similar trends.

3.2 Normal–mode Vibrational Frequencies of C₃H₅²⁺

Normal mode frequencies are tabulated for the ground–state structure **2**, with charge +2 and the 6–31+G** basis, in Table 5 at the HF, MP2 and MP4 levels.

Table 5. Normal mode frequencies, cm^{–1}, for the ground–state of **2** with charge +2, C₃H₅²⁺, and the 6–31+G** basis set

HF	MP2	MP4
172.0	211.5	203.3
314.0	335.6	343.0
423.5	446.3	431.2
773.0	844.2	824.2
981.1	908.2	909.6
1010.1	1007.2	992.5
1169.9	1106.2	1109.6
1225.0	1145.4	1143.0
1242.2	1206.6	1192.0
1330.4	1266.3	1261.4
1482.7	1380.7	1377.8
1578.7	1480.3	1478.9
1599.6	1499.5	1499.6
3215.7	3066.2	3080.8
3221.7	3098.2	3095.0
3253.8	3108.9	3104.7
3341.4	3230.9	3222.0
3345.5	3235.8	3226.5

We note that the lower frequencies tend in general to rise slightly in going from HF to MP4 levels of calculation, while higher frequencies decrease somewhat.

4 CONCLUSIONS

Our main conclusions for the geometry of $C_3H_5^{2+}$ are embodied in Figure 1, structure 2. This geometry is at MP4 level, and the changes from the HF results are modest, and therefore encouraging for the present approach. At the MP4 level, the corresponding normal mode frequencies are all real for the proposed ground-state structure and have values recorded in Table 5. The non-planar geometry shown clearly in the ‘side view’ panel of Figure 2 is in contrast to that found for the singly-charged species, the structure of which is shown, but only at MP2 level, in Figure 3. The linear structure of $C_3H_5^{2+}$ seems to be excluded, on energetic grounds. It is worth adding here that, for the doubly charged species in the ground state, the Mulliken charges at MP4 level are $\sim 0.34 - 0.40 |e|$ on each of the five H atoms, with generally smaller values on the carbon atoms. We note that Gluch *et al.* [5], in their treatment of $C_3H_5^{2+}$, carried out optimization at the MP2/aug-cc-pVTZ level. Thus their results for bond lengths, for example, are similar to, though not identical to, ours. There remains the question of studying metastable $C_3H_5^{2+}$, and its decomposition pathways and products, as considered by Gluch *et al.* [5]. This will require techniques transcending those used in the present investigation, and we are presently focusing attention on such an extension of the present study.

It is relevant to add, in relation to future work that might prove fruitful, the recent experiment of Shimizu *et al.* [7] using time-of-flight mass spectroscopy, in which Coulomb explosion of benzene induced by an intense femtosecond laser field was investigated. For orientation, the laser intensity used was $8 \times 10^6 \text{ W/cm}^2$, with pulse width 120 fs. Multiply charged ions of C^{q+} with $q = 1-4$ and H^+ were detected by these authors and their energy distribution was found to be in the range 0–160 eV. It will be an interesting theoretical investigation for the future to gain further insight into the anisotropy of the Coulomb explosion. The experimental workers [7] conclude that there is some similarity with the anisotropic Coulomb explosion of C_{60} irradiated with a femtosecond laser pulse of high intensity [8]. Again, first-principles theory is called for if one is to seek a deeper interpretation of these experimental results.

Finally, it is of interest to record here that very recent experimental work has been reported [9] on the dissociation of acetaldehyde in an intense laser field. An interpretation is given by the authors in terms of field-assisted dissociation rather than by Coulomb explosion of multicharged ions. Again, further theoretical studies are clearly called for.

Acknowledgment

IAH acknowledges support from the IWT – Flemish region under grant IWT-161. NHM wishes to acknowledge partial financial support from ONR for work on density-functional theory. Especial thanks are due to Dr. P. Schmidt of that Office for motivation and his continuing interest. CVA thanks the University of Antwerp for financial support under grant GOA-BOF-UA nr.23 and BOF UA/SFO UIA 2002. Finally, we acknowledge constructive suggestions from reviewers, which are embodied in the final version.

5 REFERENCES

- [1] F. Gobet, B. Farizon, M. Farizon, M.J. Gaillard, J. P. Buchet, M. Carré, P. Scheier, and T. D. Märk, Direct Experimental Evidence for a Negative Heat Capacity in the Liquid-to-Gas Phase Transition in Hydrogen Cluster Ions: Backbending of the Caloric Curve, *Phys. Rev. Lett.* **2002**, *89*, 183403–1–183403–4; F. Gobet, B. Farizon, M. Farizon, M. J. Gaillard, J. P. Buchet, M. Carré, and T. D. Märk, Probing the Liquid-to-Gas Phase Transition in a Cluster via a Caloric Curve, *Phys. Rev. Lett.* **2001**, *87*, 203401–1–203401–4.
- [2] I. A. Howard, F. E. Leys, N. H. March, C. Van Alsenoy, J. A. Alonso, and A. Rubio, Molecular Clusters of Hydrogen, Deuterium and Tritium: Especially Cationic Species $H_3^+(H_2)_m$: $m=2, 5$ and 14 , in: *Proceedings of the SPIE, 5118 (Nanotechnology)*, Eds. R. Vajtai, X. Aymerich, L. B. Kish and A. Rubio, SPIE, Bellingham, WA, 2003, pp. 331–339.
- [3] J. Zweiback, R. A. Smith, T. E. Cowan, G. Hays, K. B. Wharton, V. P. Yanovsky, and T. Ditmire, Nuclear Fusion Driven by Coulomb Explosions of Large Deuterium Clusters, *Phys. Rev. Lett.* **2000**, *84*, 2634–2637.
- [4] I. A. Howard, J. A. Alonso, N. H. March, A. Rubio, and C. Van Alsenoy, Coulomb Explosion of Deuterium Cationic Clusters, *Phys. Rev. A* **2003**, *68*, 065201–1 – 065201–4.
- [5] K. Gluch, J. Fedor, S. Matt-Leubner, O. Echt, A. Stamatovic, M. Probst, P. Scheier, and T. D. Märk, Kinetic-energy release in Coulomb explosion of metastable $C_3H_5^{2+}$, *J. Chem. Phys.* **2003**, *118*, 3090–3095.
- [6] GAUSSIAN 98, Revision A.7, M. J. Frisch, G. W. Trucks, H. B. Schlegel, G. E. Scuseria, M. A. Robb, J. R. Cheeseman, V. G. Zakrzewski, J. A. Montgomery, Jr., R. E. Stratmann, J. C. Burant, S. Dapprich, J. M. Millam, A. D. Daniels, K. N. Kudin, M. C. Strain, O. Farkas, J. Tomasi, V. Barone, M. Cossi, R. Cammi, B. Mennucci, C. Pomelli, C. Adamo, S. Clifford, J. Ochterski, G. A. Petersson, P. Y. Ayala, Q. Cui, K. Morokuma, D. K. Malick, A. D. Rabuck, K. Raghavachari, J. B. Foresman, J. Cioslowski, J. V. Ortiz, A. G. Baboul, B. B. Stefanov, G. Liu, A. Liashenko, P. Piskorz, I. Komaromi, R. Gomperts, R. L. Martin, D. J. Fox, T. Keith, M. A. Al-Laham, C. Y. Peng, A. Nanayakkara, C. Gonzalez, M. Challacombe, P. M. W. Gill, B. Johnson, W. Chen, M. W. Wong, J. L. Andres, C. Gonzalez, M. Head-Gordon, E. S. Replogle, and J. A. Pople, Gaussian, Inc., Pittsburgh PA, **1998**.
- [7] S. Shimizu, V. Zhakhovskii, F. Sato, S. Okihara, S. Sakabe, K. Nishihara, Y. Izawa, T. Yatsuhashi, and N. Nakashima, Coulomb explosion of benzene induced by an intense laser field, *J. Chem. Phys.* **2002**, *117*, 3180–3189.
- [8] J. Kou, V. Zhakhovskii, S. Sakabe, K. Nishihara, S. Shimizu, S. Kawato, M. Hashida, K. Shimizu, S. Bulanov, Y. Izawa, Y. Kato, and N. Nakashima, Anisotropic Coulomb explosion of C_{60} irradiated with a high-intensity femtosecond laser pulse, *J. Chem. Phys.* **2000**, *112*, 5012–5020.
- [9] M. E. Elshakre, L. Gao, X. Tang, S. Wang, Y. Shu, and F. Kong, Dissociation of acetaldehyde in intense laser field: Coulomb explosion or field-assisted dissociation? *J. Chem. Phys.* **2003**, *119*, 5397–5405.